Volume 8 Number 0105 **ISSN 1979-3898**

Journal of Theoretical and Computational Studies

Hydrodynamic Model for Non-equilibrium and Hot Electron Transport in ZnO MESFETs

H. Arabshahi

J. Theor. Comput. Stud. **8** (2009) 0105
Received: March 27th, 2009; Accepted for publication: June 4th, 2009

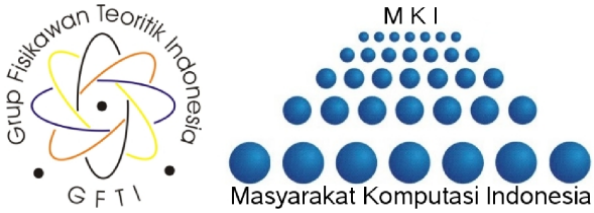

Published by

Indonesian Theoretical Physicist Group
http://www.opi.lipi.go.id/situs/gfti/

Indonesian Computational Society
http://www.opi.lipi.go.id/situs/mki/

Journal of Theoretical and Computational Studies

Journal devoted to theoretical study, computational science and its cross-disciplinary studies

URL : http://www.jurnal.lipi.go.id/situs/jtcs/

Coverage area

1. *Theoretical study* : employing mathematical models and abstractions of a particular field in an attempt to explain known or predicted phenomenon. E.g. : theoretical physics, mathematical physics, biomatter modeling, etc.
2. *Computational science* : constructing mathematical models, numerical solution techniques and using computers to analyze and solve natural science, social science and engineering problems. E.g. : numerical simulations, model fitting and data analysis, optimization, etc.
3. *Cross-disciplinary studies* : inter-disciplinary studies between theoretical study and computational science, including the development of computing tools and apparatus. E.g. : macro development of Matlab, paralel processing, grid infrastructure, etc.

Types of paper

1. *Regular* : an article contains an original work.
2. *Comment* : an article responding to another one which has been published before.
3. *Review* : an article which is a compilation of recent knowledges in a particular topic. This type of article is only by invitation.
4. *Proceedings* : an article which has been presented in a scientific meeting.

Paper Submission

The submitted paper should be written in English using the LaTeX template provided in the web. All communication thereafter should be done only through the online submission page of each paper.

Referees

All submitted papers are subject to a refereeing process by an appropriate referee. The editor has an absolute right to make the final decision on the paper.

Reprints

Electronic reprints including covers for each article and content pages of the volume are available from the journal site for free.

Indonesian Theoretical Physicist Group — Indonesian Computational Society

Secretariat Office : c/o Group for Theoretical and Computational Physics, Research Center for Physics - LIPI, Kompleks Puspiptek Serpong, Tangerang 15310, Indonesia

http://www.opi.lipi.go.id/situs/gfti/ — http://www.opi.lipi.go.id/situs/mki/

ISSN 1979-3898

J. Theor. Comput. Stud. Volume **8** (2009) 0105

Hydrodynamic Model for Non-equilibrium and Hot Electron Transport in ZnO MESFETs

H. Arabshahi
Department of Physics, Ferdowsi University of Mashhad, Mashhad, Iran

Abstract : A hydrodynamic approach is used to illustrate hot-electron and intervalley transfer effects in ZnO MESFET. The model is based on the solutions of the highly coupled non-linear partial differential equations of the full hydrodynamic model. These solutions allow to calculate the electron drift velocity and other device parameters as a function of the applied electric field. Using hydrodynamic method our calculation results show that due to the high drain current density we can expect ZnO devices have superior high power and high gain performance. Our results of numerical calculations are in fair agreement with other theoretical or experimental methods.

Keywords : hydrodynamic; intervalley; drift velocity; drain current

E-mail : arabshahi@um.ac.ir

Received: March 27th, 2009; Accepted for publication: June 4th, 2009

1 INTRODUCTION

Semiconductor device modeling includes a wide range of areas in solid state physics, applied and computational mathematics. Transport of carriers in semiconductors under applied electric field was first explained as a combination of drift due to the field, and diffusion due to concentration gradients. In the presence of high fields that change rapidly over small distances, the drift-diffusion equations, however, lose thier validity and non-local and hot-carrier effects begin to dominate device performance. In effect, apart from carrier density and velocity, carrier energy (or equivalently, temperature) needs to be considered because the carriers are not in thermal equlibrium with the lattice. In SiC and ZnO materials which are used for high-speed device design [1-4], inertia effects play an important role since the impulse and energy relaxation times of the electron gas are close to the picosecond range. The most elaborate and practicable approach for the description of charge transport in semiconductors used for device simulation would be the Monte Carlo method [5-9]. The advantage of this technique is a complete picture of carrier dynamics with reference to microscopic material parameters, e.g. effective masses and scattering parameters. But the method must be still considered as very consuming and hence not economical to be used by device designers.
Besides the simplest concept which is the traditional drift-diffusion model, there is a much more rigorous approach to the problem, namely the so-called hydrodynamic model. The hydrodynamic model we are interested in is an extension of the drift diffusion equations. It consists of a set of Euler equations with certain source terms and a Poisson equation for the electrical potential [10-14]. This model is capable of capturing some important features of semiconductor devices which are not accounted for in the classical drift-diffusion model.

Electron dynamics in compound semiconductors is determined by the multivalley band structure of the conduction band and scattering processes which include intravalley and intervalley scattering. The intravalley processes may consist of intravalley phonon, ionized impurity and electron-electron scattering, which conserve the number of electrons in the valley. However, the intervalley processes provide electron population, energy and momentum exchanges between non-equivalent valeys. In compound semiconductor such as ZnO, the lowest conduction band includes a central valley and several satellite valleys where the energy separations between valley minima are much greater than the phonon energy and the valley minima are situated in various locations in the Brillouin zone. In addition, the electron effective mass in each valley is significantly different from the others. Therefore, electrons in different valleys should be considered as different species, and transport be-

haviour of electrons in each valley at the kinetic level in the semiclassical regime is determined by distribution function. The Boltzmann transport equation in various valleys are coupled through intervalley scattering that introduces exchanges of electron population, energy and momentum between valleys. Consequently, the hydrodynamic description for electron behaviour in each valley is given by a set of hydrodynamic equations, and the hydrodynamic equations in various valleys are coupled through intervalley transitions. At high electric fields, a large number of electrons are hot enough to overcome the energy separation between central and satellite valleys. In this case, the frequent intervalley scattering dominates the scattering processes, and it therefore significantly influences nonequilibrium transport phenomena of electrons. To accurately describe nonequilibrium hot electron transport phenomena at the hydrodynamic level, a set of multivalley hydrodynamic equations that is capable of properly including exchanges of electron population, energy and momentum between valleys is thus necessary.

This paper is organised as follows. In section 2, we give a short definition of the hydrodynamic model for ZnO structure. It is emphasized that a analysis of the physical features of the charge carrier transport models is the basis for a clear understanding of their limits of applicability. In section 3 results of hydrodynamic model in ZnO MESFET are interpreted.

2 BASIC EQUATIONS

The single-gas hydrodynamic equations have been carried out to simulate the electron transport properties in ZnO MESFET. Our programe was performed using an analytical band structure model. The equations for each valley are, however, coupled through collision terms. The corresponding relaxation rates may be of the order of a picosecond and are therefore relatively large. The hydrodynamic model equations consist of the continuity equation,

$$\frac{\partial n}{\partial t} + \vec{\nabla} \cdot \vec{j} = 0, \tag{1}$$

for unipolar devices it is possible to neglect charge carrier generation and recombination term so the momentum balance equation given by [11],

$$\frac{\partial \vec{p}}{\partial t} + (\nabla p)v + (p\nabla)v = -en\vec{E} - \nabla(nkT) - \frac{\vec{p}}{\tau_p}, \tag{2}$$

or alternatively (only for x-component),

$$\frac{\partial[m^*(\epsilon')n\ \vec{v_x}]}{\partial t} + \nabla[m^*(\epsilon')nv_x v] = -qn\ \vec{E_x} - \frac{\partial(nkT)}{\partial x} - \frac{m^*(\epsilon')n\ \vec{v_x}}{\tau_p(\epsilon')}, \tag{3}$$

and the energy balance equation is

$$\frac{\partial \epsilon}{\partial t} + \nabla(v\epsilon) = -qnv\ \vec{E} - \nabla(nkTv) - \nabla(-k\nabla T) - \frac{\epsilon - \frac{3}{2}nkT_L}{\tau_\epsilon(\epsilon')}, \tag{4}$$

where n, ϵ (ϵ'=ϵ/n), and v are the electron density, the electron energy density (average electron energy) and the electron drift velocity, respectively. $\vec{v_x}$ is the x-component of the electron drift velocity and $\vec{p}=\ m^*n\ \vec{v}$ is the momentum density. Correspoding equations are valid for the y and z components. T is the electron temperature and $\epsilon_0' = 3/2kT_L$ is the average termal equilibrium energy of electrons, where T_L is the lattice temperature. The electronic current density $\vec{j}$ inside the active device is $\vec{j}=-ne\ \vec{v}$, so the total current density is,

$$\vec{j}_{\,t} = -ne\ \vec{v} + \epsilon_0\epsilon_r\frac{\partial\ \vec{E}}{\partial t}. \tag{5}$$

The momentum relaxation time $\tau_p(\epsilon')$ is related to the mobility of the electrons via $\mu(\epsilon') = em^*(\epsilon')\tau_p(\epsilon')$, and the energy relaxation time $\tau_\epsilon(\epsilon')$ describes the exchange of energy between the heated electron gas and the lattice. τ_p and τ_ϵ and the effective electron mass m^* are assumed to be functions of the mean electron energy.

The hydrodynamic equations, together with Poisson's equation,

$$\Delta\phi = -\ \vec{\nabla}\ E = -\frac{e}{\epsilon_0\epsilon_r}(N_d^+ - n), \tag{6}$$

form a complete set of equations that can be used to solve for the electron density, velocity, energy and electric field for given boundary conditions. A closing relation for the mean electron energy ϵ', the electron temperatute T and velocity $\vec{v}$ is,

$$\epsilon' = \frac{1}{2}m^*(\epsilon')v^2 + \frac{3}{2}kT + \beta_U(\epsilon')\Delta E_{\Gamma U}. \tag{7}$$

The last term in equation 7 accounts for the fact that a minimum energy of about $\Delta E_{\Gamma U}$=1.5 eV is necessary to excite an electron from central Γ-valley to the

nearest upper valley. β_U is the relative fraction of electrons in the upper valley for the stationary homogeneous case. The term $\beta_U(\epsilon')\Delta E_{\Gamma U}$ is often neglected, but this may lead to an overestimation of the electron temperature of more than 1000 K at high energies.

In our simulated model time discretization is used for all the hydrodynamic equations by forward Euler differencing method. The discretization is always written down only for the x-component of vectorial quantities in the sequel, since the corresponding expressions for y-components are then easy to drive. The simplest method for assigning charged particles to cells is the nearest-grid-point scheme in which the total charge found in a cell is assigned to the midpoint of that cell. After each sampling Poisson's equation is solved and the electric field is updated. Poisson's equation is solved by a combined fast Fourier transform [15] and Buneman cyclic reduction method [16-17] developed by Walmsley and Abram [18]. This calculational scheme is integrated with a capacity matrix approach [17] that facilitates the use of individual rectangular regions to form more complicated structures. Poisson's equation is expressed in discrete form as a set of three-point finite difference equations.

After setting all the material and device parameters, the simulation is started in a state of charge neutrality everywhere in the device. The simulated particles are distributed appropriately among all the mesh cells to achieve the required neutrality. In the two-dimensional device models used here there is no variation of electron density or electric field normal to the $x-y$ plane and scaler quantities at a timestep like electron density $n^t_{i,j}$, energy $\epsilon^t_{i,j}$, temperature $T^t_{i,j}$ and potential $\phi^t_{i,j}$, are located at the center of the cells, whereas vectorial quantities like the electric field components $E^t_{x;i+\frac{1}{2},j}$, $E^t_{y;i+j+\frac{1}{2}}$ or the velocity components $v^t_{x;i+\frac{1}{2},j}$, $v^t_{y;i+j+\frac{1}{2}}$ are always calculated first at midpoint between the scaler quantities. For example, we can define for electric field the following intermediate value as,

$$E_{x;i,j} = \frac{1}{2}(E_{x;i-\frac{1}{2},j} + E_{x;i+\frac{1}{2},j}). \tag{8}$$

The fundamental quantities are calculated using boundary conditions at each timestep. For example the momentum balance equation is discretized in the following form,

$$\begin{aligned}\frac{p^{t+1}_{x;i+\frac{1}{2},j} - p^t_{x;i+\frac{1}{2},j}}{\Delta t} &= -qn^t_{i+\frac{1}{2},j}E^t_{x;i+\frac{1}{2},j} \\ &-\frac{k}{\Delta x}(n^t_{i+1,j}T^t_{i+1,j} - n^t_{i,j}T^t_{i,j})n^t_{i+\frac{1}{2},j} \\ &-(p^t_{x;i+\frac{1}{2},j}v_{x;i+\frac{1}{2},j} - p^t_{x;i-\frac{1}{2},j}v_{x;i-\frac{1}{2},j})/\Delta x \\ &-(p^t_{x;i+\frac{1}{2},j}v_{y;i,j+\frac{1}{2},j} - p^t_{x;i+\frac{1}{2},j-1}v_{y;i,j-\frac{1}{2}}/\Delta y \\ &-p^t_{x;i+\frac{1}{2},j}/\tau^t_{p;i+\frac{1}{2},j},\end{aligned} \tag{9}$$

where $p_{x;i+\frac{1}{2},j} \geq 0$ and $p_{y;i,j+\frac{1}{2}} \geq 0$ and the same discretization are used in y direction of the electron velocity as well. From the momentum density we can obtain the new particle current density by,

$$j^{t+1}_{x;i+\frac{1}{2},j} = p^{t+1}_{x;i+\frac{1}{2},j}m^*_{i+\frac{1}{2},j}, \tag{10}$$

and the momentum density at (i,j) is extrapolated from neighbouring points in the direction of the electron flow x-component,

$$\begin{aligned}p^{t+1}_{x;i,j} &= \frac{3}{2}p^{t+1}_{x;i-\frac{1}{2},j} - \frac{1}{2}p^{t+1}_{x;i-\frac{3}{2},j} \quad : \quad p^{t+1}_{x;i+\frac{1}{2},j} \geq 0 \\ p^{t+1}_{x;i,j} &= \frac{3}{2}p^{t+1}_{x;i+\frac{1}{2},j} - \frac{1}{2}p^{t+1}_{x;i+\frac{3}{2},j} \quad : \quad p^{t+1}_{x;i+\frac{1}{2},j} \leq 0,\end{aligned} \tag{11}$$

and finally we have,

$$v^{t+1}_{x;i,j} = p^{t+1}_{x;i,j}n^t_{i,j}m^{*t}_{i,j}, \tag{12}$$

$$v^{t+1}_{x;i+\frac{1}{2},j} = j^{t+1}_{x;i+\frac{1}{2},j}n^t_{i+\frac{1}{2},j}m^{*t}_{i+\frac{1}{2},j}. \tag{13}$$

The electron temperature is related to the energy density by the relation $\epsilon^t_{i,j} = \frac{3}{2}n^t_{i,j}kT^t_{i,j} + \frac{1}{2}m^*_{i,j}n^t_{i,j}(v^{2t}_{x;i,j} + v^{2t}_{y;i,j}) + \beta^t_{U;i,j}\Delta E_{\Gamma U}$ and can assume to be dependent variable. The upwind discretization of the energy balance equation is given by,

$$\begin{aligned}\frac{\epsilon^{t+1}_{i,j} - \epsilon^t_{i,j}}{\Delta t} &= -en^t_{i,j}(v^{t+1}_{x;i,j}E^t_{x;i,j} + v^{t+1}_{y;i,j}E^t_{y;i,j}) \\ &-\frac{\epsilon^t_{i,j} - \frac{3}{2}n^t_{i,j}kT_L}{\tau^t_{\epsilon;i,j}} \\ &-(j^t_{x;e,i+\frac{1}{2},j} - j^t_{x;e,i-\frac{1}{2},j})/\Delta x \\ &-(j^t_{x;p,i+\frac{1}{2},j} - j^t_{x;p,i,i-\frac{1}{2},j})/\Delta x \\ &-(j^t_{x;h,i,j+\frac{1}{2}} - j^t_{x;h,i-\frac{1}{2},j})/\Delta x \\ &-(j^t_{y;e,i,j+\frac{1}{2},j} - j^t_{y;e,i,j-\frac{1}{2}})/\Delta y \\ &-(j^t_{y;p,i,j+\frac{1}{2}} - j^t_{y;p,i,j-\frac{1}{2}})/\Delta y \\ &-(j^t_{y;h,i,j+\frac{1}{2}} - j^t_{y;h,i,j-\frac{1}{2}})/\Delta y,\end{aligned} \tag{14}$$

where the energy current density is defined as,

$$j^t_{x;e,i+\frac{1}{2},j} = v^{t+1}_{x;i+\frac{1}{2},j}\epsilon^t_{i+\frac{1}{2},j}, \tag{15}$$

$$j^t_{x;p,i+\frac{1}{2},j} = kj^{t+1}_{x;i+\frac{1}{2},j}T^t_{i+\frac{1}{2},j}, \tag{16}$$

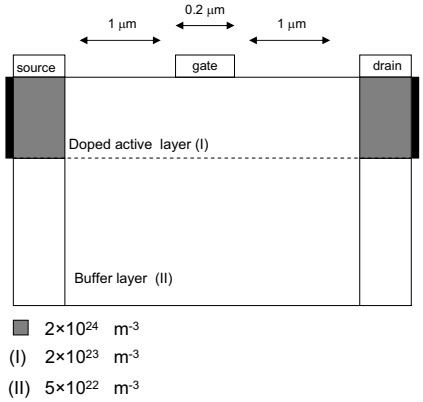

FIGURE 1: The two-dimensional model of ZnO MESFET. The modelled structure is divided into three regions, as indicated. Electron particles are initially distributed keeping all regions charge neutral. The location of the source and the drain implants and the top and back buffer layer are marked.

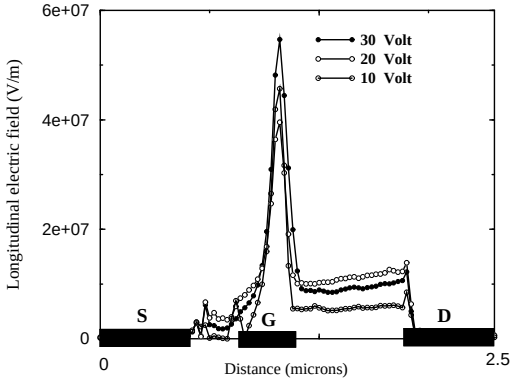

FIGURE 2: longitudinal electric field throught the simulated device for various source-drain bias when the gate voltage is -1 V at $T = 300$ K.

and,

$$j^t_{x;h,i+\frac{1}{2},j} = k^t_{i+\frac{1}{2},j}(T^t_{i+1,j} - T^t_{i,j})/\Delta x. \qquad (17)$$

Using the calculated mean electron energy, the other electron transport parameters are also updated. Also, using the particle current density $j = nev$, the current continuity equation is discretized in a conservative way as,

$$\frac{n^{t+1}_{i,j} - n^t_{i,j}}{\Delta t} = -(j^t_{x;,i+\frac{1}{2},j} - j^t_{x;i-\frac{1}{2},j})/\Delta x - (j^t_{y;,i+j+\frac{1}{2}} - j^t_{y;i,j-\frac{1}{2}})/\Delta y. \qquad (18)$$

The particles that leave cell (i,j) in x-direction enter cell $(i+1,j)$ and analogously for the y-direction.

3 CALCULATION RESULTS

Fig. 1 shows a schematic of the modelled ZnO MESFET. The overall device length is 2μm in the x-direction and the device has a 0.2μm gate length and 0.15μm source and drain length. The source and drain have ohmic contacts and gate is in Schottky contact in 1 eV to represent the contact potential at Au/Pt. The source and drain regions are doped to 2×10^{24} m^{-3} electron concentration and the top and down buffer layers are doped to 2×10^{23} m^{-3} and 5×10^{22} m^{-3} electron concentration, respectively.

The device is simulated at room temperature. In order to obtain stable and physically meaningful results, the field cell size used for the central region of the simulated MESFET is 20×1 nm^2 (horizontal$\times$vertical), but that in high doped source and drain regions is finer (5×1 nm^2).

Fig. 2 shows the longitudinal electric field for various source-drain bias when the gate voltage is -1 V. The longitudinal electric field plotted in figure 2 shows the high electric field in the region under the gate where the hot electrons are seen to exist in the upper valley due to attaining enough energy to be scattered into the satellite conduction valley.

Figs. 3 and 4, respectively, show the steady-state Γ-valley band profile and the total electron density as a function of distance from the source when the drain-source potential drop is 20 V and the gate voltage is -1 V. Note that almost all the drain-source potential is dropped within the gate-drain region of the channel, leaving a flat potential profile near the source and drain. As electrons move towards the drain, they lose potential energy and gain sufficient kinetic energy to transfer to the upper conduction valleys where their drift velocity is reduced. Figure 4 demonstrate the electron density through the device. The gate depletion region is clearly seen where the electron density is several orders of magnitude lower than it is near the source and drain.

Fig. 5 shows electron transport data recorded through the source-drain section when the source-drain bias is 20 V and the gate voltage is -1 V especifically, the variations of Γ-valley band profile, drift velocity, average electron kinetic energy and the total electron density throughout the simulated device. The average electron velocity reaches about 2×10^5 ms^{-1} and then declines towards the drain. The steep decrease in the average kinetic energy on the drain side of the gate is due to the transfer of electrons to the upper valley. The electron density through the device is shown in figure 5d. The gate depletion region is clearly seen where the electron density is several or-

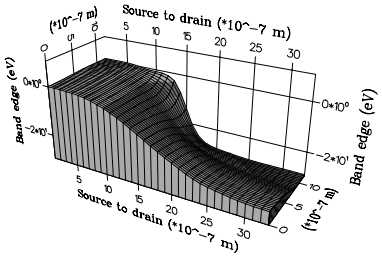

FIGURE 3: Interpolated contour plot showing the steady-state Γ-valley band profile through the simulated ZnO MESFET at room temperature when the bias applied to the gate is -1 V and the drain-source bias is 20 V.

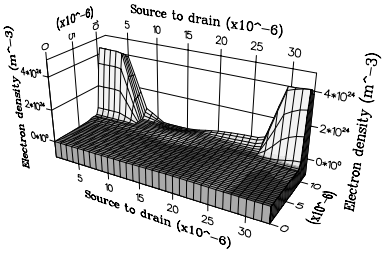

FIGURE 4: Electron density throughout the modelled region of the ZnO MESFET when the bias applied to the gate is -1 V and the drain-source bias is 20 V.

ders of magnitude lower than it is near the source and drain.

CONCLUSIONS

A hydrodynamic model was used to model steady-state electron transport in a ZnO metal semiconductor field effect transistor. Our calculation results show that due to the high drain current density we can expect ZnO devices have superior high power and high gain performance.

ACKNOWLEDGMENTS

This work benefited from useful discusions with M. G. Paezi.

JTCS

REFERENCES

[1] D. C. Look, D. C. Reynolds, J. R. Sizelove, R. L. Jones, C. W. Litton, G. Cantwell and W. C. Harsch, *Solid-State Commun.* **105** 399 (1998)

[2] S. H. Kim, J. S. Lee and H. C. Choi, *IEEE Electron Device Lett.* **20** 113 (1999)

[3] K. Vanheusden, W. L. waren, C. H. Seager, D. R. Tallant, J. A. Voigt and B. E. Gnade, *J. Appl. Phys.* **79** 7983 (1996)

[4] J. F. Wagner, *Science* **300** 1245 (2003)

[5] J. Nishii, A. Ohtomo, K. Ohtani, H. Ohno, and M. Kawasaki, *Jpn. J. Appl. Phys.* **40** L1193 (2005)

[6] K. Ueno, I. H. Inoue, H. Akoh, M. Kawasaki, Y. Tokura, and H. Takagi, *Appl. Phys. Lett.* **83** 1755 (2003)

[7] R. J. Trew, M. W. Shin and V. Gatto, *Solid-State Electronics.* **41** 1561 (1997)

[8] B. E. Foutz, L. F. Eastman, U. V. Bhapkar and M. Shur, *Appl. Phys. Lett.* **70** 2849 (1997)

[9] T. Kurosawa, *J. Phys. Soc. Jpn.*, **21**, 424 (1966)

[10] C. Moglestue, *Monte Carlo Simulation of Semiconductor Devices 1993* pub. Chapman and Hall

[11] C. Jacoboni and P. Lugli, *The Monte Carlo Method for semiconductor and Device Simulation 1989* pub. Springer-Verlag

[12] H. Arabshahi, M. R. Benam and B. Salahi *Modern Physics Letters B.* **21**, 1715 (2007)

[13] H. Arabshahi, *Modern Physics Letters B.* **21**, 199 (2007)

[14] J. W. Cooley and J. W. Tukey, *Mathematics of Computation.* **19**, 297, (1965)

[15] G. D. Bergland, *Mathematics of Computation.* **21**, 236, (1967)

[16] G. D. Bergland, *Mathematics of Computation.* **22**, 275, (1968)

[17] C. Temperton, *Journal of Computational Physics.* **34**, 314, (1980)

[18] M. Walmsley and R. A. Abram, *The international Journal for Computation and Mathematics.* **15**, 31, (1996)

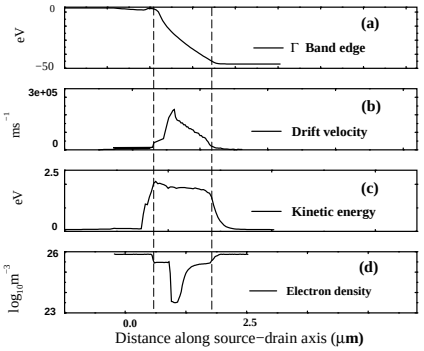

FIGURE 5: Electron transport characteristics as a function of position in the model ZnO MESFET. (a) Γ-valley band profile,(b) Average drift velocity, (c) Average kinetic energy and (d) Electron density when the bias applied to the gate is -1 V and the drain-source bias is 20 V.